Oil & Natural Gas Technology

DOE Award No.: DE-FE0028895

Quarterly Research Performance Progress Report (Period ending 3/31/2017)

Dynamic Behavior of Natural Seep Vents: Analysis of Field and Laboratory Observations and Modeling

Project Period (10/01/2016 to 09/30/2017)

Submitted by:
Scott A. Socolofsky

Texas A&M Engineering Experiment Station
DUNS #:847205572.
3136 TAMU
College Station, TX 77843-3136
e-mail: socolofs@tamu.edu
Phone number: (979) 845-4517

Prepared for:
United States Department of Energy
National Energy Technology Laboratory

April 30, 2017

Office of Fossil Energy

DISCLAIMER:

Contents

List of Figures

List of Tables

1 Accomplishments

1.1 Summary of Progress Toward Project Objectives

The *overarching goal* of this project is to develop a computer model to predict the trajectory and dissolution of hydrate-armored methane bubbles originating from natural seeps. The model is based on the Texas A&M Oilspill Calculator (TAMOC), developed by Dr. Socolofsky, and which will be refined and validated through this project to explain fundamental laboratory and field observation of methane bubbles within the gas hydrate stability zone of the ocean water column. *Our approach* is to synthesize fundamental observations from the National Energy Technology Laboratory's (NETL) High-Pressure Water Tunnel (HPWT) and field observations from the Gulf Integrated Spill Research (GISR) seep cruises (cruises G07 and G08), conducted by the PIs in the Gulf of Mexico, to determine the dissolution pathways and mass transfer rates of natural gas bubbles dissolving in the deep ocean water column. We will achieve these objectives by pursuing the *following specific objectives*:

1. Analyze existing data from the NETL HPWT.

2. Synthesize data from the GISR natural seep cruises.

3. Refine and validate the seep model to predict available data.

4. Demonstrate the capability of the seep model to interpret multibeam data.

Ultimately, the *main outcome and benefit* of this work will be to clarify the processes by which hydrate-coated methane bubbles rise and dissolve into the ocean water column, which is important to predict the fate of methane in the water column, to understand the global carbon cycle, and to understand how gas hydrate deposits are maintained and evolve within geologic and oceanic systems, both at present baselines and under climate-driven warming.

The work accomplished during this reporting period focused on the first two specific objectives. We have completed the transfer all of the HPWT data (about 24 TB) from NETL to a new server installed at Texas A&M University. We have also begun analysis of this data, focusing in this period on the bubble shrink rate, the hydrate formation time, organization of the data into slow-speed and high-speed image sequences, and evaluating the high-speed data to understand the interface mobility. For the GISR field data, we have been developing analysis tools for the acoustic data collected during the cruises (G07 and G08), specifically, was have been comparing the predictions

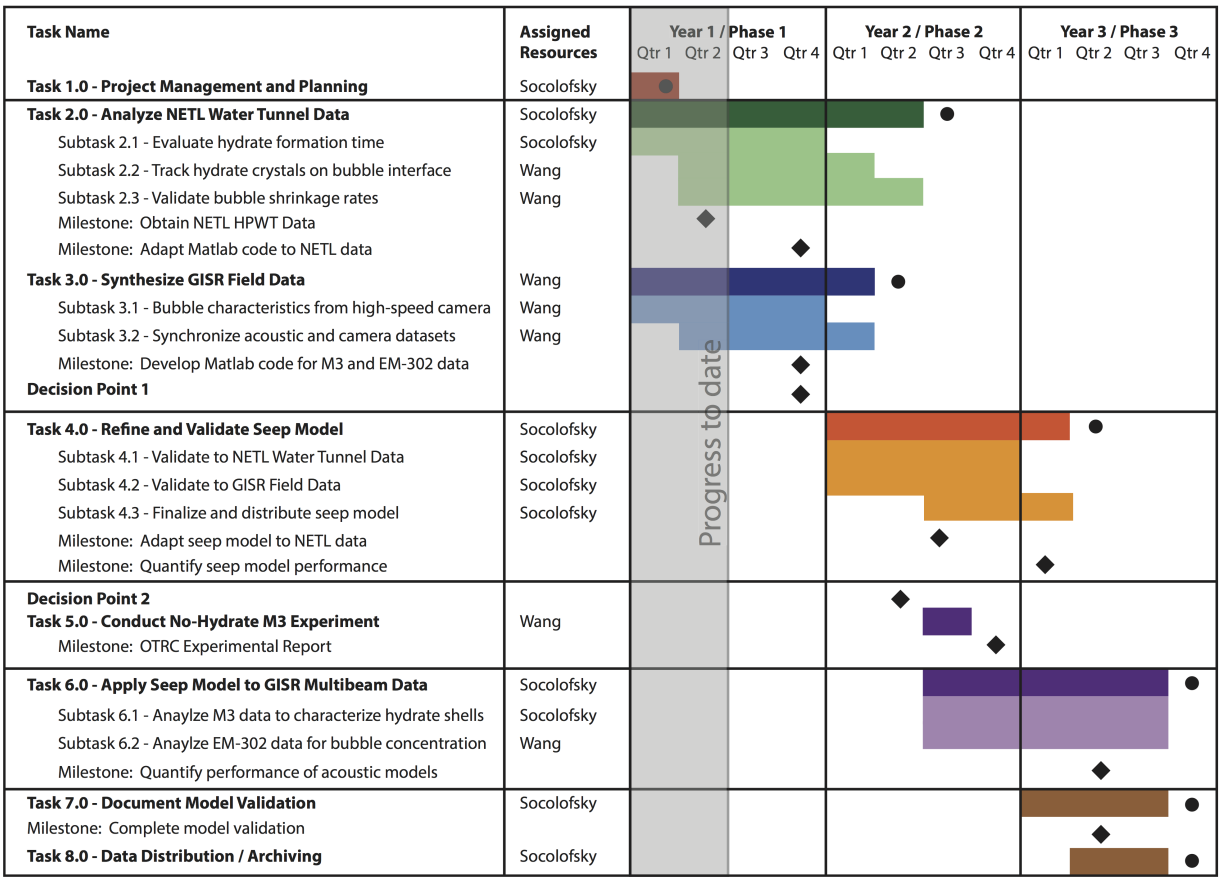

Figure 1: Project Timeline.

for target strength from our numerical model with the measured unspecified backscatter data from the EM 302 multibeam echosounder.

1.2 Progress on Research Tasks

Figure 1 presents the project timeline, showing each of the project tasks, subtasks, and milestones as identified in the Project Management Plan (PMP). The present reporting period concludes the second quarter of FY 2017 (Phase 1 of the project). During this period, we completed Milestone 1 (Obtain NETL HPWT Data), and made progress on each subtask of Tasks 2 and 3. The work conducted on these tasks during this reporting period is summarized in the following sections, organized by each Task.

1.2.1 Task 1.0: Project Management Planning

The Project Management Plan was completed during the first quarter of Phase 1.

1.2.2 Task 2.0: Analyze NETL Water Tunnel Data

In this project, we will analyze the comprehensive data set of HPWT data collected by NETL. To do this, we have transfered a complete copy of all raw data (primarily image files) to Texas A&M University and have installed this data on a secure internal server. This work was completed on March 24, 2017, and achieved Milestone 1 for the project (Obtain NETL HPWT Data). The sections below summarize our progress during the present reporting period in analyzing this data.

Subtask 2.1 - Evaluate Hydrate Formation Time

The complete set of image data for the HPWT experiments allows an analysis of the kinetics of hydrate formation on methane bubbles under different pressure and temperature. To perform this analysis, we analyze the image data for each experiment and identify image frames where the hydrate characteristics change. We can then compare these morphological changes to the conditions in the tank to understand the dynamics of hydrate formation on the bubble-water interface.

Figure 2 presents a summary of the pressure and temperature in the HPWT throughout a complete experiment. In this experiment, hydrate initially formed, the hydrate shell then underwent transformation, was melted by releasing the pressure, and then reformed by increasing the pressure a second time. In the figure, we identify several green diamonds (A-R), which represent specific times where the bubble-hydrate morphology changed or times that document the bubble characteristics immediately preceding a change in the experimental conditions (temperature or pressure).

Figures 3 to 5 show images of the bubbles at each of the green diamond points in Figure 2. Initially, the bubble is free of hydrate at point A, immediately after the pressure is increased to 10 MPa at 8.8°C, a point within the hydrate stability region. Images B to C show the rapid formation of a hydrate shell (see also the inset for times during this period in Figure 2). At point D, the hydrate has fully formed, and the bubble appears rigid in the images, wobbling and meandering in the countercurrent. Point H documents the bubble-hydrate conditions just before the pressure is slowly decreased back to about 7.1 MPa, the Images I through L document the gradual dissolution of the hydrate into floating crystals. At point M, the hydrate has not fully dissociated, the pressure is reduced further to 6.9 MPa, and Image N shows an apparently hydrate-free bubble. A hydrate skin is reformed at Point P by increasing the pressure to 8.8 MPa. The hydrate skin appears to become more opaque (thickening, perhaps) as the pressure is further increased back to 8.6 MPa at Point R (refer to the second inset for the pressure versus time during this last phase of the experiment).

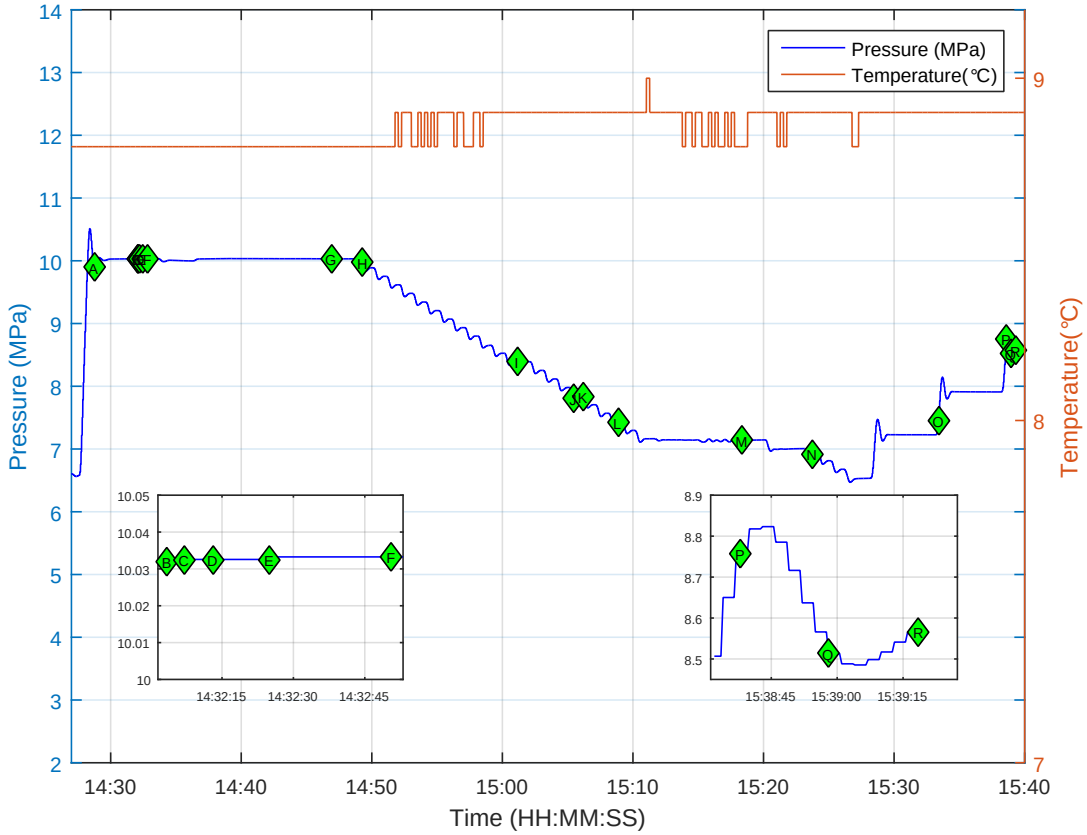

Figure 2: An example of time series of ambient conditions for a bubble before, during, and after hydrate formation.

We will analyze all of the experimental runs in this same way, capturing images and tank conditions at all major morphology changes or tank operational conditions changes. Once we have this data, we will extract hydrate formation times at different pressure, temperature, and operational conditions (e.g., initial formation at the start of an experiment or re-formation after dissociation as experiments progress). This data will be a key calibration and validation parameter in Phase 2 of this project, when we adapt our hydrate formation model to predict these data. Over 300 different experiments were conducted in the HPWT; this analysis of those data will continue through the remaining quarters of Phase 1.

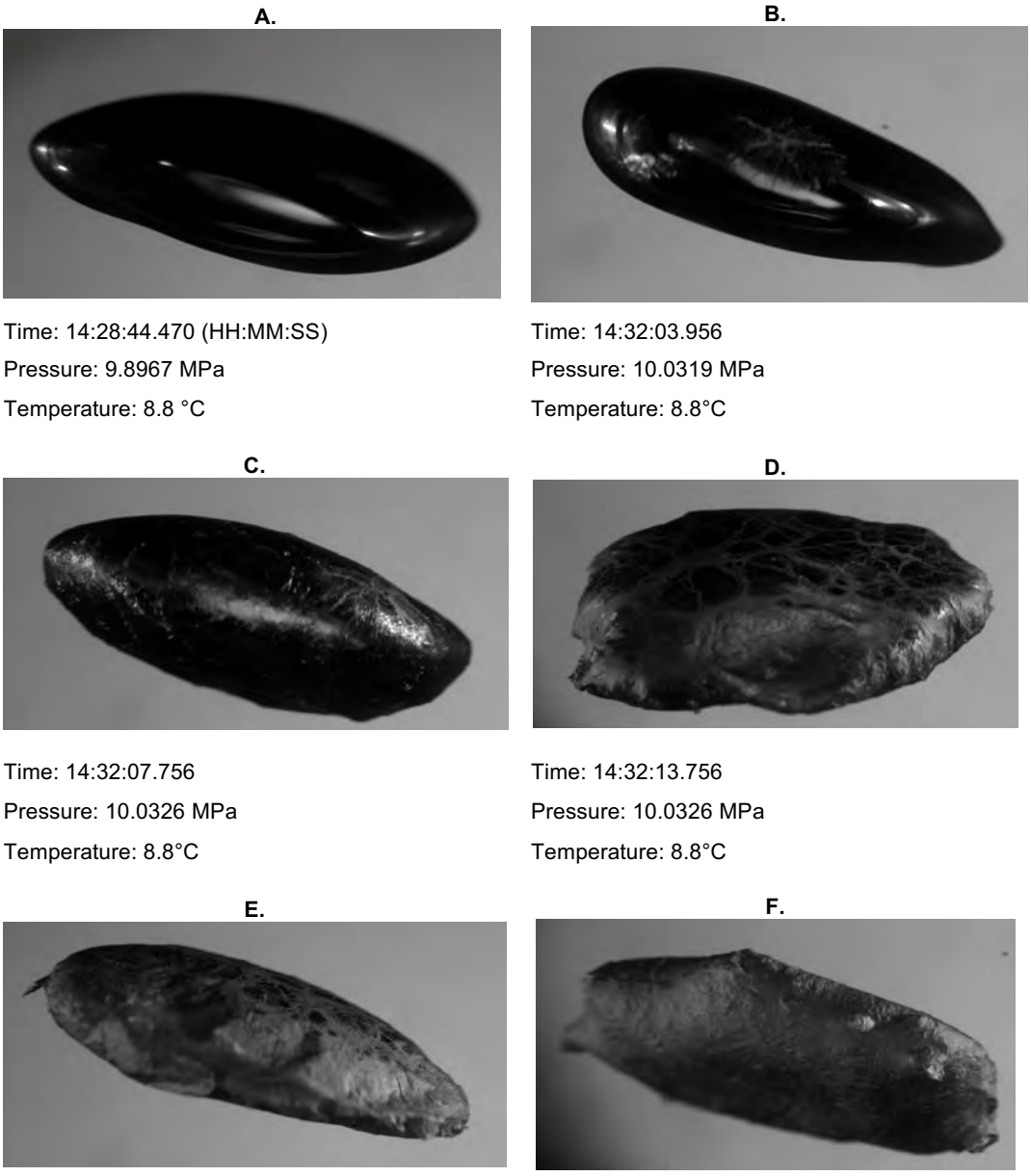

Figure 3: An example of morphological change of a bubble before, during, and after hydrate formation. The selection of A-F is shown in Figure 2.

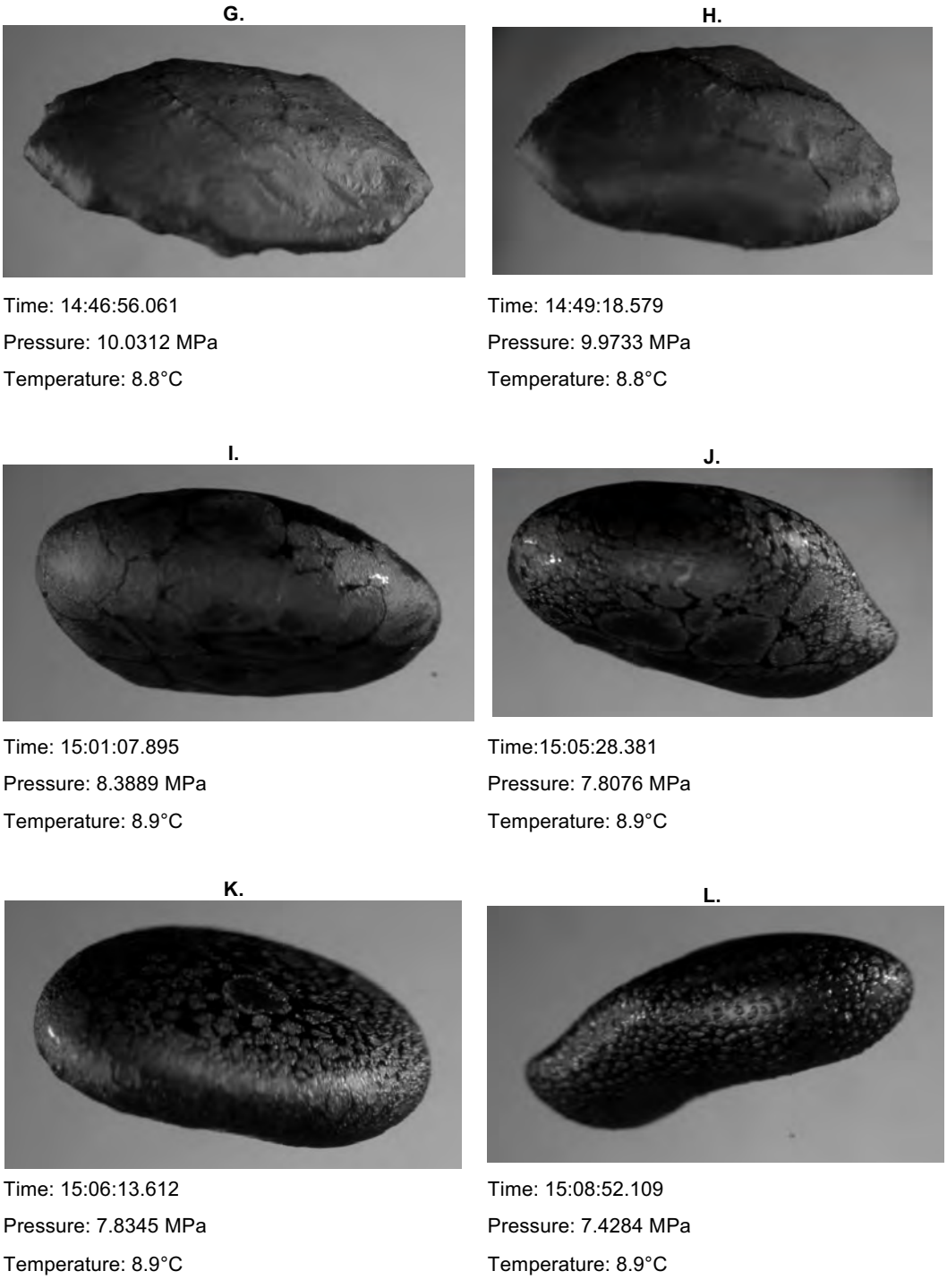

Figure 4: An example of morphological change of a bubble after hydrate formation during dissolution and pressure changes. The selection of G-L is shown in Figure 2.

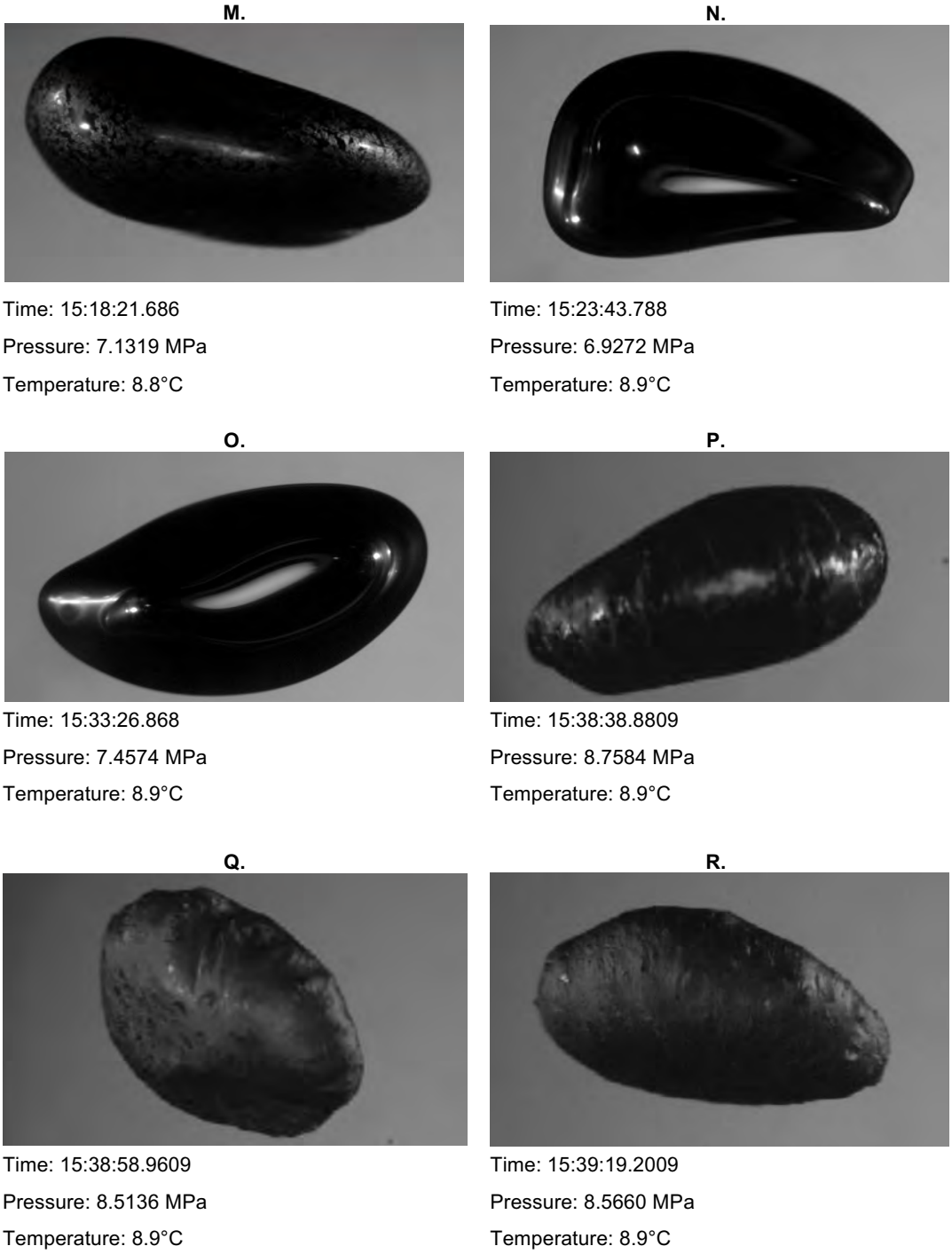

Figure 5: An example of morphological change of a bubble under varying pressure and temperature. The selection of M-R is shown in Figure 2.

Subtask 2.2 - Track Hydrate Crystals on Bubble Interface

Two types of image data were collected in the HPWT experiments. One camera recorded at a relatively low frame rate (about 15 fps) and recorded continuously for the entire duration of the experiment. A second camera recorded at high frame rates (up to 1000 fps), but could only record short time sequences (order a few seconds). After a short image sequence was collected, the data had to be downloaded from the camera before another image sequence could be collected. Hence, there are a few high-speed image sequences collected per each experiment, with at least 5 minutes between high-speed image burst. Also, it appears that the high-speed camera did not exist during the early experiments so that high-speed image data are only available for a subset of the complete experimental matrix.

To track the motion of hydrate crystals on the bubble-water interface, only the high-speed data can be used. Through communications with Franklin Shaffer at NETL, he shared several videos clips they had analyzed to determine the fractional area of coverage by hydrate during the period where hydrate has not yet covered the whole bubble. By watching these videos, it is clear that the hydrate crystals in some of the high-speed images are moving and can be tracked. We will begin working on these analyses in the next two performance periods. This work is important because mass transfer rates are much higher for mobile interfaces than for immobile interfaces. If hydrate crystals are moving around on the bubble-water interface, then mass transfer rates (dissolution) may be high during this phase of the hydrate dynamics.

Subtask 2.3 - Validate Bubble Shrinkage Rates

Bubble size and shape can be evaluated from both the slow-speed and high-speed data. The slow-speed data are used to determine the overall shrinkage rate of the bubbles due to dissolution, and the high-speed data can be used to understand the time-scales of bubble oscillations and rotations. A sample from both of these datasets was analyzed during the present reporting period.

Slow-speed Image Data. In the existing DOE reports, the slow-speed camera data have been analyzed for bubble size, and the shrinkage rate of bubbles for each of the experiments were reported (Warzinski et al. 2014, Levine et al. 2015). In this Subtask, we will adapt our Matlab image processing tools to the HPWT data and validate the bubble size data reported in these existing reports.

During the present reporting period, we analyzed two full time series of bubble shrinkage data. Figure 6 presents an analysis of bubble shrinkage data for a bubble without any hydrate skin. The

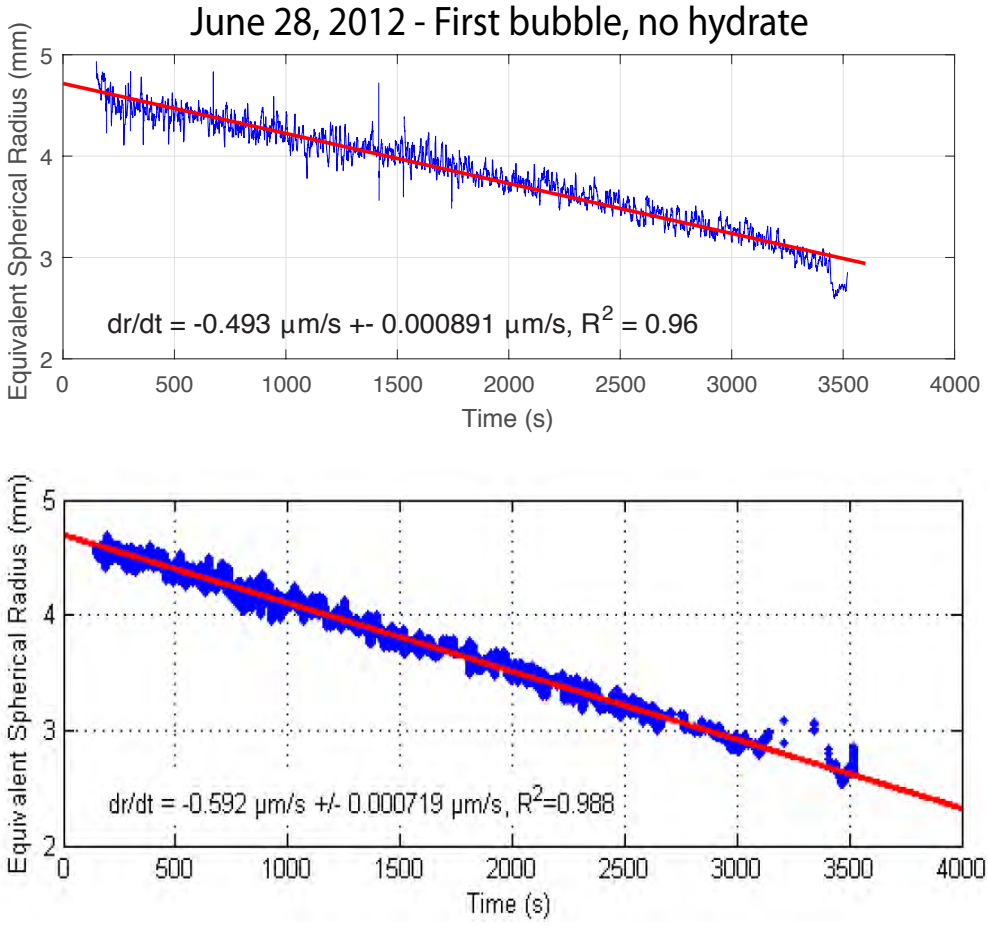

Figure 6: Comparison of bubble size shrinkage between our result (top panel) and the previously reported result (bottom panel). 1st bubble, no hydrate, June 28, 2012.

top panel presents the result from our Matlab code; the bottom panel presents the result from the DOE reports for the same image sequence. Comparing the two sets of data it is clear that our Matlab code is returning the same bubble sizes as reported in the DOE reports. The DOE report data shows less variability. We searched the data archive to follow their image analysis method and determined that they apply a moving average (typically of 100 frames) to smooth variability in the individual measurements.

In Figure 6, we did not apply a moving average for our predictions (top panel). Comparing the shrinkage rates reported by our Matlab code to that in the DOE reports shows that our shrinkage rates are slower (-0.49 μm/s compared to -0.59 μm/s in the DOE report). This is explained as follows. The images in the raw data were not captured with a constant frame rate. The actual time for each image frame is displayed in each image, but there is no time stamp in the image or movie

file meta data. It is clear that the DOE report used the actual time stamp for each image when computing their shrinkage rate, which is the correct approach to employ. So far, we have not been able to automatically read the frame times from the images; hence, our data is based on assuming a uniform frame rate over the entire image sequence. This leads to a bias in our current result.

The important conclusion from this data analysis comparison so far is that 1.) our Matlab image processing codes return the same sizes as were measured and reported for the DOE reports, 2.) the DOE reports applied a moving average to smooth large excursions in the bubble size data, which does not affect estimates of the bubble shrinkage rate, 3.) because the images were not captured at a constant frame rate, the true image capture times are needed to estimate a precise bubble shrinkage rate, and 4.) the DOE report used the correct image capture times; hence, we agree with the bubble sizes and shrinkage rate data published in those reports.

Figure 7 presents a similar comparison of our image processing methods to those used in the DOE reports for a bubble with hydrate shell. This was a shorter image sequence than in Figure 6 and had a much more uniform image capture rate. The agreement between our data and the reported data is again very close, and our computed shrinkage rates are within the error bounds reported in the DOE report. Therefore, again, we agree with the bubble shrinkage rate data published in the DOE reports.

In the coming quarter, we will work to extract the image frame times so that we can have an exact comparison between our image processing tools and the results in the DOE reports. This must be automated because, for instance, for the data in Figure 6, there are 60,000 images, making it impossible to obtain image time stamps by hand. We will also tabulate all of the shrinkage rate data from the DOE reports to produce an analyzed set of data for these experiments.

High-speed Image Data. A second high-speed camera captured the evolution of the bubbles in the HPWT for short sequences spaced randomly throughout the complete experiments. These high-speed data show interfacial waves on the bubbles, rotations of the bubbles, and motions of hydrate crystals on the bubble-water interface prior to full hydrate coverage or during hydrate dissociation.

During the present reporting period, we analyzed one of these high-speed image sequences to obtain the bubble size for a non-hydrated bubble as a function of time. Figure 8 shows the results of our image analysis code for bubble size and bubble aspect ratio. Because the raw camera data are available for these high-speed image sequences, the true capture time of each image is also

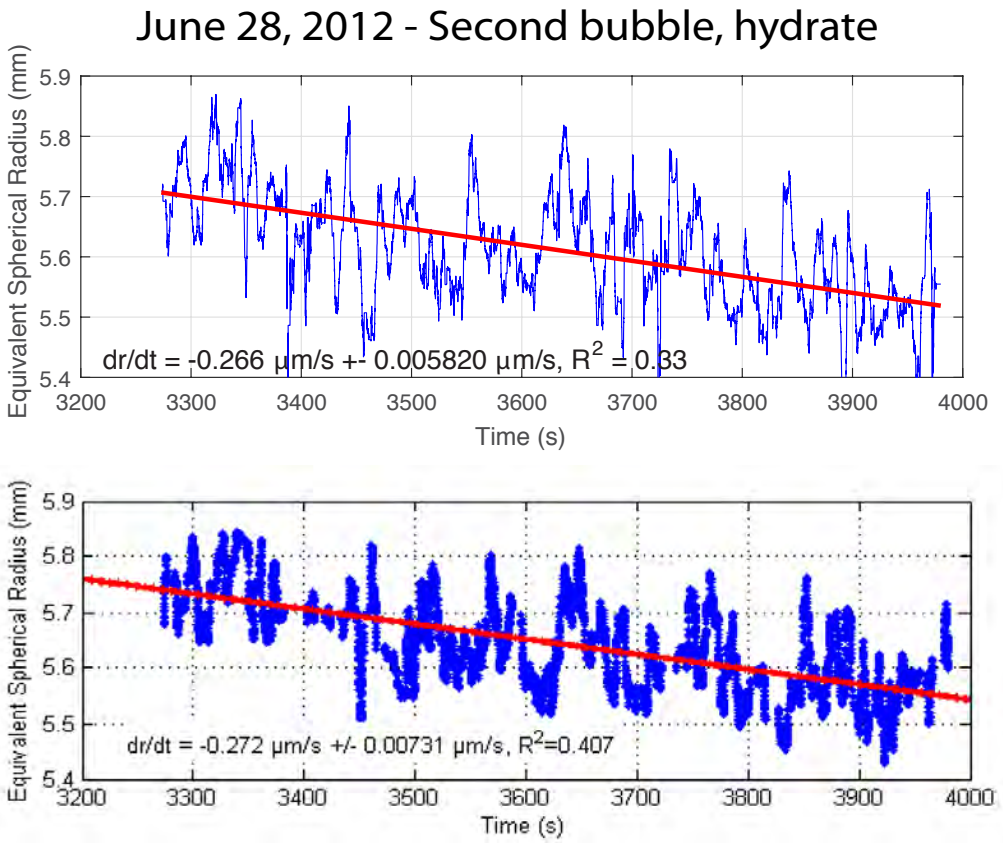

Figure 7: Comparison of bubble size shrinkage between our result (top panel) and the previously reported result (bottom panel). 2nd bubble, with hydrate, June 28, 2012.

known. Hence, there is no uncertainty in the measurement time of each frame. These time series show two major oscillation frequencies: a very fast oscillation with a period of about 1/8 s and a slower frequency of period 2 to 3 seconds. The fast oscillation is due to interfacial waves traveling on the bubble-water interface and the slower oscillation corresponds to rotation or migration in the field of view.

We analyzed the spectral information in these time series to quantify the oscillation frequencies more rigorously. Figure 9 presents the results of this analysis. We calculated the power density spectrum and the cross-correlation spectrum and phase for both the bubble size data and the bubble aspect ratio. The peak frequency of the short-period oscillations is clearly shown in both the bubble and aspect ratio power spectra, and covers a frequency range of 7 to 9 Hz (with a period of 1/8 s in the center). Both the bubble size and aspect ratio show this same peak, indicating the waves traveling on the bubble-water interface give rise to different estimates of bubble size as they

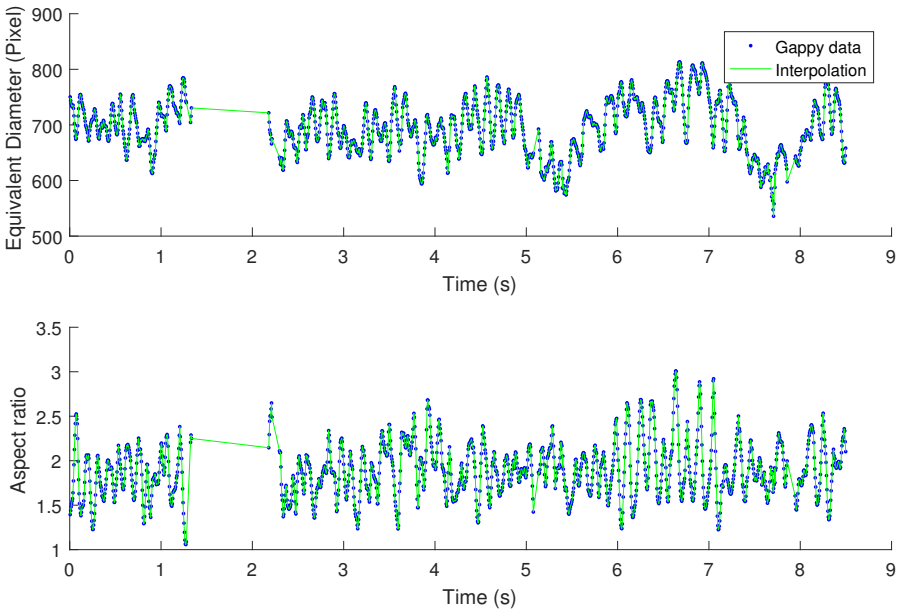

Figure 8: Time series of bubble diameter (top panel) and aspect ratio (bottom panel) for a single high-speed camera sequence. Data for video 2012-06-29_Set2_FlashCine10.

traverse the bubble. The cross-spectrum also shows strong correlation at this same peak frequency. From the cross-power phase, it is clear that bubble size and aspect ratio are about 180 degrees out of phase, which indicates that the bubble size is consistently measured to be largest when the aspect ratio appears small. Small aspect ratios conform closer to spherical bubbles; however, the out-of-plane shape remains unknown, so it is not possible to give a definitive estimate of bubble volume using these single-camera measurements.

We plan to use the high-speed imagery in two ways. First, we will compare the power spectral data for bubbles with and without a hydrate skin. Because the hydrate skin freezes the bubble-water interface, effectively eliminating interfacial waves, we expect the wobbling peak in the power spectrum to shift or disappear. Second, we will explore models of interfacial waves on bubbles to determine whether the characteristics modes of the bubble shape can be matched to these oscillation frequencies. In that case, it may be possible to obtain more accurate estimates of bubble volume. Both of these activities will be ongoing through future reporting periods.

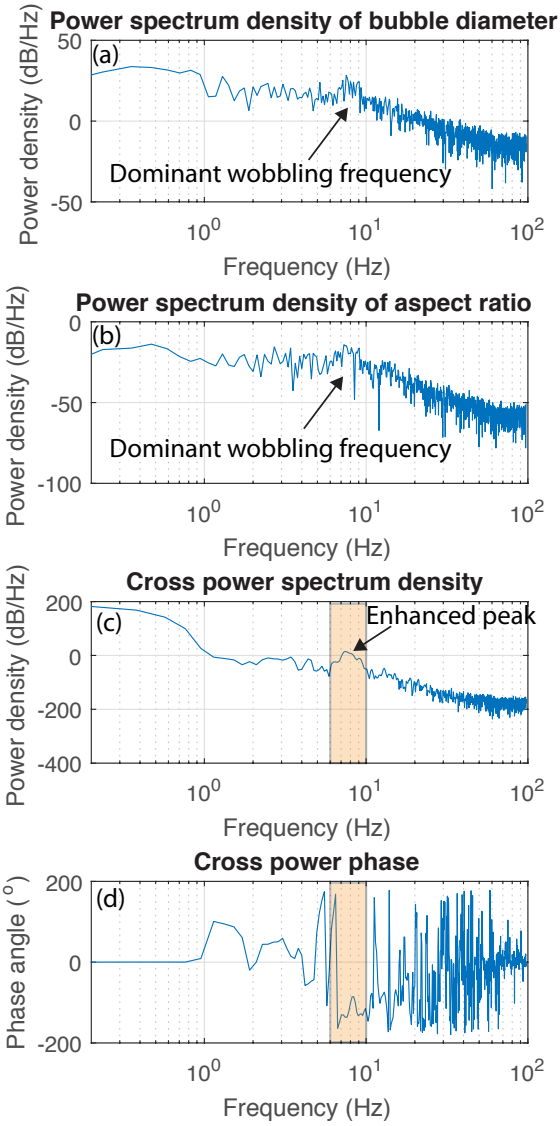

Figure 9: Sample spectral analysis of bubble diameter and aspect ratio for the high-speed data in Figure 8: (a) Power spectrum density of bubble diameter, (b) Power spectrum density of aspect ratio, (c) Cross spectrum density of bubble diameter and aspect ratio, where the orange box shows the enhanced peak where coherence of signals of bubble diameter and aspect ratio, (d) Cross spectrum phase shows the phase lag between two signals at the coherent frequency region.

Progress Toward Milestones

Milestone 1 (Obtain NETL HPWT Data) was completed on March 24, 2017. The other major milestone for Task 2 is to adapt our image analysis codes in Matlab to analyze the image data in the HPWT Dataset. The results presented above show that our Matlab code is working and producing similar results to the NETL analyses for bubble size. We will continue to adapt our codes to track hydrate crystals and to use the codes to analyze the complete dataset. We are on-track to complete this next milestone within Phase 1 as planned.

1.2.3 Task 3.0: Synthesize GISR Field Data

The project PIs conducted two research cruises to natural seeps in the Gulf of Mexico under funding to the GISR consortium. These were the G07 cruise in July 2014 to Mississippi Canyon (MC) block 118 and to Green Canyon (GC) block 600 and the G08 cruise in April 2015 to MC 118. Both cruises were on the *E/V Nautilus* and utilized the remotely operated vehicle (ROV) *Hercules*. This project utilizes two main datasets from these cruises: data from our stereoscopic high-speed camera system mounted on the ROV (Wang et al. 2015) and acoustic data collected by an M3 sonar mounted on the ROV and an EM-302 multibeam sonar mounted on the haul of the ship. The image data from the G07 cruise was analyzed previously and reported in Wang et al. (2016). This project will analyze all of the acoustic data and complete analysis of the image data for the G08 cruise. The sections below summarize our progress during the present reporting period in analyzing this field data.

Subtask 3.1 - Bubble Characteristics from High-Speed Camera.

In our previous progress report, we showed significant progress toward results for this subtask. Effort during the current reporting period was focused on other subtasks.

Subtask 3.2 - Synchronize Acoustic and Camera Datasets.

There are two main sets of acoustic data from the GISR cruises. In our previous progress report, we showed work for the data from the M3 multibeam sonar, which was mounted on the ROV. During the present reporting period, we focused our work on the EM 302 multibeam sonar, mounted in the haul of the *E/V Nautilus*.

The EM 302 records unspecified amplitude of backscatter, and the Fledermaus Water Column Module software package can be used to process this data to obtain the unspecified amplitude of

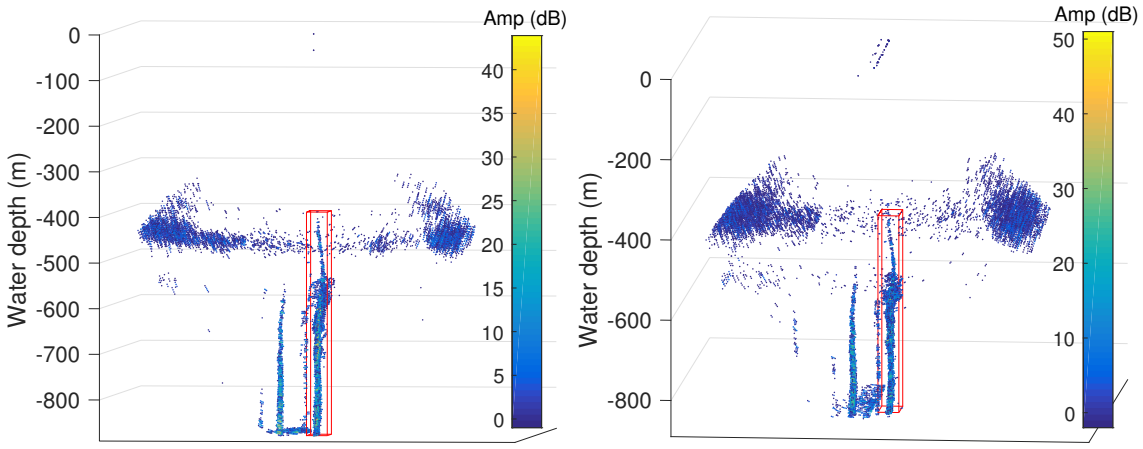

Figure 10: The unspecified amplitude of backscatter from natural seeps at MC 118 on July 18, 2014. The red box indicates the primary seep flare. The two subfigures show the data during two different ship tracks.

backscatter in the water column. We have captured snapshots from the EM 302 dataset for each time the ship passed over the main seeps we surveyed on these cruises, and we isolated the water column signature of each seep from the background noise and the signatures of other neighboring seeps. Figure 10 shows an example for the main seep in MC 118 for two ship tracks on July 18, 2014. The red column highlights the region in space where the bubbles from that seep are present, and the blue water column returns give the measured acoustic data for that seep. This data must be extracted for each ship pass and will be used in Phase 2 of this project to validate predictions of our natural seep numerical model.

One way to utilize this data for validation is to compare the measured target strength from the EM 302 with the predicted target strength from the numerical model for a simulation of the seep. Figure 11 presents one means to post-process the acoustic data and a comparison with the numerical prediction. In the post-processing method, we take the statistics of all of the acoustic data at each water depth and compute the mean and standard deviation (shown as the blue points and error bars in the right panel of Figure 11). The red line is the predicted target strength when taking the numerical model output and using an analytical prediction for acoustic backscatter for the data (following methods in Weber et al. 2014). The shape and relative magnitudes of both curves are in good agreement. However, the simulated data has to be shifted by 30 dB in order to match the actual measured amplitudes. Because the EM 302 is uncalibrated, this is an expected problem.

We had a conference call with Tom Weber, who is funded by DOE NETL under the Fate of

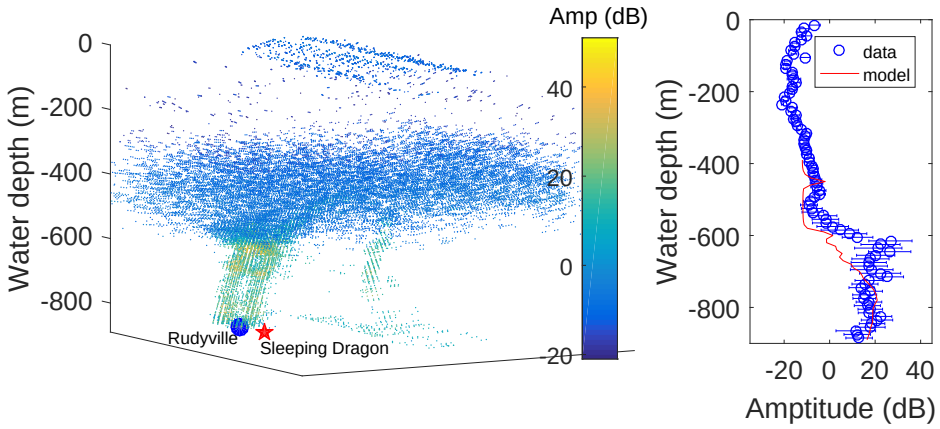

Figure 11: Left panel: the measured unspecified acoustic backscatter amplitude on July 18, 2014 at site MC 118. Right panel: vertical profile comparison between measured unspecified backscatter amplitude and the simulated total target strength. The symbols and errorbars indicate the mean and standard deviation of the measurement data. The simulated data was offset by 30 dB to match the measured unspecified data.

Methane in the Water Column (see External Collaborators, below) to discuss these results and gain feedback on other potential approaches. Dr. Weber explained to us that there are existing algorithms from Kongsberg that can be used to convert the unspecified acoustic backscatter to target strength, taking into account range and other important environmental parameters. He agreed that our current approach was reasonable, but that it would be better to replace our unspecified backscatter data with the computed target strength. We are currently working on those calculations and will update the results in this section in our next progress report.

Progress Toward Milestone

The major milestone for Task 3 is to create a Matlab analysis program that can use the TAMOC model together with the acoustic data to infer bubble properties for bubbles observed in the acoustics. Our approach follows an approach by Weber et al. (2014), and we have continued to develop our analysis code during the present reporting cycle, where we have focused on the EM 302 datasets.

1.3 Deliverables

To date, we have completed the following list of deliverables:

1. **Project Management Plan (PMP)**. The PMP was delivered in its accepted and final form on October 28, 2016.

2. **Data Management Plan (DMP)**. No revisions were requested by the Project Officer to the plan submitted with the proposal; hence, the original DMP is the present guiding document. Revisions will be updated as necessary throughout the project as required by the Project Officer.

In the present reporting period, no new deliverables were due. The next set of deliverables include complete archives of the analysis data produced through analysis of the HPWT and GISR Seep Cruise data. Progress toward these deliverables is summarized above in the reporting for each Task.

1.4 Milestones Log

Table 1 presents the schedule of milestones with their verification methods for the duration of the project period. Milestone 1 was due during the present reporting period and was also completed. See Section 1.2 for details on progress toward completion of up-coming milestones.

1.5 Plans for the Next Reporting Period

Work for the next reporting period will continue on Tasks 2 and 3 (refer to Figure 1). For Task 2, we will continue to analyze the bubble size data by reading the image time stamps from the slow-speed camera data. We will also analyze the spectral information for the remaining high-speed image time series for bubble size and shape and will begin to track hydrate crystals on the bubble-water interface.

For Task 3, we will continue to work on the EM 302 datasets to convert the unspecified backscatter data to target strength and to compare target strength predictions from our numerical model with the measured data. We will also continue to draft a journal paper to report the results of the G08 cruise. Our target journal for this article is *Geophysical Research Letters*.

Table 1: Milestones schedule and verification methods.

	Milestone	**Completion Date**	**Comments**
Title	Acquisition of NETL HPWT data		
Date Completed	March 24, 2017		
Verification Method	Email verification		
Title	Adapt Matlab code to NETL data		
Planned Date	September 2017		
Verification Method	Report		
Title	Matlab code for M3 and EM-302 data		
Planned Date	September 2017		
Verification Method	Report		
Title	OTRC Experimental Report		
Planned Date	August 2018		
Verification Method	Report		
Title	Adapt seep model to NETL data		
Planned Date	June 2018		
Verification Method	Report		
Title	Quantify seep model performance		
Planned Date	December 2018		
Verification Method	Report		
Title	Quantify performance of acoustic models		
Planned Date	March 2019		
Verification Method	Report		

References

Clift, R., J. R. Grace, and M. E. Weber (1978), *Bubbles, drops, and particles*, Academic Press.

Fisher, H. B., E. J. List, R. C. Y. Koh, J. Imberger, and N. H. Brooks (1979), *Mixing in inland and coastal waters*, Academic Press.

Okubo, A. (1971), Oceanic diffusion diagrams, *Deep Sea Research and Oceanographic Abstracts*, *18*(8), 789–802.

Levine, J., I. Haljasmaa, R. Lynn, F. Shaffer, and R. P. Warzinski (2015), Detection of Hydrates on Gas Bubbles during a Subsea Oil/Gas Leak, NETL-TRS-6-2016, EPAct Technical Report Series, U.S. Department of Energy, National Energy Technology Laboratory: Pittsburgh, PA.

Rehder, G., I. Leifer, P. G. Brewer, G. Friederich, and E. T. Peltzer (2009), Controls on methane bubble dissolution inside and outside the hydrate stability field from open ocean field experiments and numerical modeling, *Marine Chemistry*, *114*(1-2), 19–30.

Wang, B., and S. A. Socolofsky (2015), A deep-sea, high-speed, stereoscopic imaging system for in situ measurement of natural seep bubble and droplet characteristics, *Deep Sea Research Part I*, *104*, 134–148.

Wang, B., S. A. Socolofsky, J. A. Breier, and J. S. Seewald (2016), Observation of bubbles in natural seep flares at MC 118 and GC 600 using in situ quantitative imaging, *Journal of Geophysical Research: Ocean*, *121*, 2203–2230.

Warzinski, R. P., F. Shaffer, R. Lynn, I. Haljasmaa, M. Schellhaas, B. J. Anderson, S. Velaga, I. Leifer, and J. Levine (2014), The role of gas hydrates during the release and transport of well fluids in the deep ocean, DOI/BSEE Contract E12PG00051/M11PPG00053, Final Report, U.S. Department of Energy, National Energy Technology Laboratory.

Weber, T. C., L. Mayer, K. Jerram, J. Beaudoin, Y. Rzhanov, and D. Lovalvo (2014), Acoustic estimates of methane gas flux from the seabed in a 6000 km(2) region in the northern gulf of mexico, *Geochemistry Geophysics Geosystems*, *15*(5), 1911–1925.

2 Products

2.1 Publications, Conference Papers, and Presentations

There were no new items to report during this performance period.

2.2 Websites or Other Internet Sites

The natural seep model used for this project, the Texas A&M Oilspill Calculator (TAMOC), is published via an open source code sharing service at:

http://github.com/socolofs/tamoc

2.3 Technologies or Techniques

Nothing to report.

2.4 Inventions, Patent Applications, and/or Licenses

Nothing to report.

2.5 Other Products

Nothing to report.

3 Participants and other collaborating organizations

3.1 Project Personnel

- 1. **Name**: Scott A. Socolofsky
  2. **Project Role**: Principal Investigator
  3. **Nearest person months worked during reporting period**: 1
  4. **Contribution to Project**: Overall project management and direction. Dr. Socolofsky has led the collection of the HPWT data, directed the data analysis methods, and completed all project reporting requirements.
  5. **Collaborated with individual in foreign country**: No
  6. **Travelled to foreign country**: No

- 1. **Name**: Binbin Wang
  2. **Project Role**: Co-Principal Investigator
  3. **Nearest person months worked during reporting period**: 2
  4. **Contribution to Project**: Analyzed the image data for the G08 cruise, created model for acoustic data from M3 sonar and EM-302 multibeam, and compared the measured data to model results from TAMOC. He also trained the Ph.D. student to begin analysis of the NETL HPWT data.
  5. **Collaborated with individual in foreign country**: No
  6. **Travelled to foreign country**: No

- 1. **Name**: Byungjin Kim
  2. **Project Role**: Ph.D. Student
  3. **Nearest person months worked during reporting period**: 3
  4. **Contribution to Project**: Organized the HPWT data, summarized the existing results from the NETL reports, and analyzed HPWT data for bubble size, hydrate formation time, and bubble interface mobility.
  5. **Collaborated with individual in foreign country**: No
  6. **Travelled to foreign country**: No

3.2 Partner Organizations

None to report.

3.3 External Collaborators or Contacts

This project works in close collaboration with researchers in the DOE/NETL funded project "Fate of Methane in the Water Column," led by the U.S. Geological Survey (USGS) in Woods Hole (Carolyn Ruppel), and with a new project led by the University of Rochester (John Kessler) to advance understanding of the environmental implications that methane leaking from dissociating gas hydrates could have on the ocean-atmosphere system. Dr. Socolofsky visits and communicates with researchers in these projects regularly and shares updates on work in progress. Accomplishments associated with these collaborations are detailed in Section 1.

4 Impact

None at this point.

5 Changes / Problems

Personnel. The project hired a Ph.D. Student beginning January 2017. This is a delay of three months from the original project plan. This delay occurred because the proposal for this project was written after the recruiting season for Ph.D. students for fall 2017 was already complete. This short delay of three month in starting a Ph.D. student on the project has not delayed performance in any of the current project tasks. We anticipate that we may request carry-forward of budgeted Ph.D. student salary and tuition at the end of Phase 1, and we may need to request a no-cost extension of up to three months at the end of the project.

Data. There were several problems to overcome in transferring the HPWT data to Texas A&M University. The main problem was that half of the hard drives provided by NETL to Texas A&M were encrypted when they arrived in College Station. We shipped these drives back and forth at least twice before reformatting the drives at NETL and rewriting them solved the problem. Because half of the data arrived on time and readable, this did not delay progress on Task 2, but did delay slightly the completion of Milestone 1. The milestone was completed during this performance period and no net delay or impact on the project is anticipated.

6 Special Reporting Requirements

None required.

7 Budgetary Information

Table 2 summarizes expenditures for the current phase of the project. The current, reported spending is lower than actual because the co-PI, Binbin Wang, could not immediately be charged to the project. His title changed at Texas A&M University, which required written permission from the project manager at DOE NETL to bill his time. This approval was received, and we immediately submitted a payroll correction to move his salary charges to this project. However, because of the timing of the correction, the approval chain has not yet completed. After the payroll correction, project spending for both PIs should be on track. The remaining project spending will

slightly lag the budget throughout Phase 1 due to the fact that the Ph.D. student was not hired in Q1, but rather started in Q2.

Table 2: Budget Report

	Budget Period 1							
Baseline Reporting	**Q1**		**Q2**		**Q3**		**Q4**	
Quarter	10/1/16 - 12/31/16		1/1/17 - 3/31/17		4/1/17 - 6/30/17		7/1/17 - 9/30/17	
DE-FE0028895	Q1	Cumulative Total	Q2	Cumulative Total	Q3	Cumulative Total	Q4	Cumulative Total
Baseline Cost Plan								
Federal Share	$33,752	$33,752	$29,716	$63,468	$27,810	$91,278	$53,034	$144,312
Non-Federal Share	$12,029	$12,029	$12,029	$24,058	$8,019	$32,077	$4,009	$36,086
Total Planned	$45,781	$45,781	$41,745	$87,526	$35,829	$123,355	$57,043	$180,398
Actual Incurred Cost								
Federal Share	$11,037	$11,037	$22,617	$33,654				
Non-Federal Share	$12,029	$12,029	$12,029	$24,058				
Total Incurred Costs	$23,066	$23,066	$34,646	$57,712				
Variance								
Federal Share	$-22,715	$-22,715	$-7,099	$-29,814				
Non-Federal Share	$0	$0	$0	$0				
Total Variance	$-22,715	$-22,715	$-7,099	$-29,814				